

# 闭式热泵干燥介质温湿度演化及对能耗的影响

Medium temperature and humidity evolution of closed heat pump drying  
and its influence on energy consumption

于贤龙<sup>1,2</sup>贾振超<sup>1,2</sup>慈文亮<sup>1,2</sup>张宗超<sup>1,2</sup>赵 峰<sup>1,2</sup>YU Xian-long<sup>1,2</sup> JIA Zhen-chao<sup>1,2</sup> CI Wen-liang<sup>1,2</sup> ZHANG Zong-chao<sup>1,2</sup> ZHAO Feng<sup>1,2</sup>

(1. 山东省农业机械科学研究院,山东 济南 250100;

2. 农业农村部黄淮海现代农业装备重点实验室,山东 济南 250100)

(1. Shandong Academy of Agricultural Machinery Sciences, Jinan, Shandong 250100, China;

2. Huang Huai Hai Key Laboratory of Modern Agricultural Equipment, Ministry of Agriculture  
and Rural Affairs, P.R.China, Jinan, Shandong 250100, China)

**摘要:**目的:解析闭式热泵干燥过程中物料脱水、干燥介质温湿度与耗能间的交互作用。方法:在60℃、10%RH的控制参数下,通过试验确定物料脱水特性、干燥介质温湿度演化及系统组件耗能。结果:干燥前期物料脱水速率较快,干燥1.5 h后物料脱除了整个干燥过程96%的水分;该阶段空气介质的相对湿度维持在24%以上,水分经蒸发器表面快速冷凝并排出,除湿能耗比最高可达1.03 kg/kW;热泵机组是干燥过程的主要耗能部件,其功耗随干燥介质温度的升高而升高;受干燥介质相对湿度降低和外部循环排热的影响,除湿能耗比在干燥后期迅速下降,在2 h后仅为0.004 kg/kW。结论:热泵干燥的能量利用与介质温湿度有密切关系,在物料含水率较高时干燥具有高除湿能耗比,而在干燥后期会随介质相对湿度值迅速下降;恒定的温湿度控制方法不利于闭式热泵系统在干燥后期的节能。

**关键词:**闭式热泵;除湿干燥;介质温湿度;除湿能耗比

**Abstract: Objective:** This study aimed to resolve the interactions among the material dehydration, temperature and humidity of dry medium, and the energy consumption. **Methods:** The dehydration characteristics, temperature and humidity evolution of dry medium, and energy consumption of system component

had been determined by testing under control parameters of 60 °C and 10% RH. **Results:** Dehydration rate of the materials was relatively fast in the early stage, 96 percent of the moisture was removed from the material after 1.5 hours of drying. At this stage, the relative humidity of drying medium remained above 24 percent, the moisture in drying medium was rapidly condensed and discharged from the surface of the evaporator, and the maximum value of specific moisture extraction ratio was 1.03 kg/kW. Heat pump unit was the main energy consuming part in the drying process, and its power increased with the temperature of the drying medium. The specific moisture extraction ratio decreased rapidly in the later drying stage, and its value was only 0.004 kg/kW after 2 hours. **Conclusion:** The energy utilization of heat pump drying was closely related to the temperature and humidity of medium and moisture content of material. Drying had a high specific moisture extraction ratio when the moisture content of material was high, and fell off as the relative humidity decrease. The constant temperature and humidity control method was not suitable for the energy saving of the closed heat pump system in the later drying stage.

**Keywords:** closed heat pump; dehumidification drying; temperature and humidity of medium; specific moisture extraction ratio

**基金项目:**山东省农业科学院农业科技创新工程(编号:CXGC2022E16);国家自然科学基金项目(青年基金)(编号:32201691);山东省自然科学基金(编号:ZR2019PEE047)

**作者简介:**于贤龙,男,山东省农业机械科学研究院工程师,博士。通信作者:张宗超(1985—),男,山东省农业机械科学研究院工程师,硕士。E-mail:617196821@qq.com

赵峰(1972—),男,山东省农业机械科学研究院研究员,硕士。E-mail:zf@sjlaser.com

**收稿日期:**2022-06-27 **改回日期:**2022-10-10

干燥作为农产品加工中高能耗操作环节,提质增效一直是其发展的重要方向,降低加工能耗对于干燥行业发展具有重要意义<sup>[1]</sup>。热泵干燥是一种最具节能优势的干燥技术,能够输出比运行耗能更多的热能<sup>[2]</sup>。作为热泵系统的一种,闭式除湿系统在运行过程中无需与外界环境进行气体交换,通过蒸汽冷凝方式排出物料蒸发出的水分<sup>[3]</sup>。与开放式系统相比,闭式热泵干燥系统具有

热效率高、系统独立的优点<sup>[4]</sup>。目前,闭式热泵干燥被广泛应用于粮食<sup>[5]</sup>、果蔬<sup>[6]</sup>、水产品<sup>[7]</sup>等农产品干燥领域。

闭式热泵干燥设备由热泵机组与干燥系统两大部分组成,空气介质是干燥系统与热泵机组传热传质的媒介。干燥介质的状态受热泵系统和物料状态共同控制,同时作用于物料脱水和热泵装置运行,进而影响物料水分蒸发速率和热泵除湿能耗比<sup>[8]</sup>。由于物料在干燥过程中含水率跨度较大,传热传质过程存在明显的非线性特征<sup>[9]</sup>。单一的干燥控制方式不利于物料脱水与品质形成,会造成能量的不合理投入<sup>[10]</sup>。闭式干燥系统具有较高的产热比,但除湿能耗比却低于半开放式热泵系统。Tunckal 等<sup>[11]</sup>在香蕉片闭式热泵干燥研究中发现,43 ℃干燥温度下,热泵系统的能效比达到 3.059,但单位能耗除湿量仅为 0.212 kg/(kW·h)。

针对闭式热泵干燥除湿能耗比低的问题,研究拟解析闭式热泵干燥装置干燥过程的除湿能耗比、空气介质温湿度的演化与物料脱水的相关关系,探究各耗能部件在干燥过程中的耗能规律,以期为闭式热泵干燥装置与控制系统开发提供依据。

## 1 材料与方法

### 1.1 试验装置

如图 1 所示,闭式热泵干燥试验箱由热泵机组、辅助加热装置、干燥室、循环风机组成。物料平铺于干燥室料盘中,通过热风对流实现干燥。

如图 2 所示,热泵机组含有两个冷凝器,压缩机、冷凝器 1、膨胀阀 1、蒸发器组成冷媒内循环,实现干燥介质的除湿与加热。循环风机推动空气介质自下而上穿过干燥室,与物料接触后的湿空气经顶部返回蒸发器完成冷凝除湿,干空气经冷凝器完成再加热。压缩机、冷凝器 2、

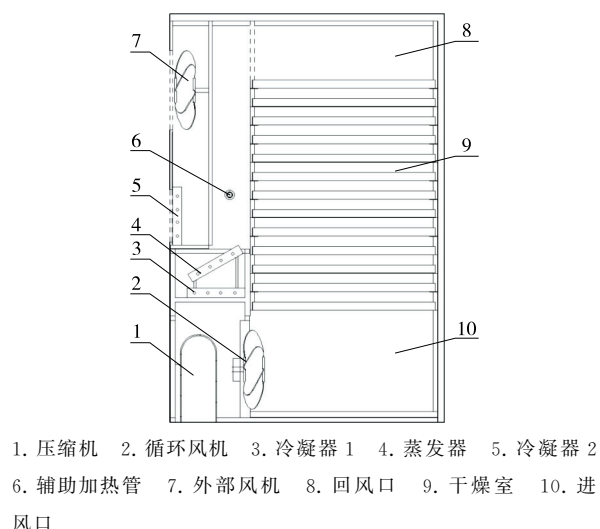


图 1 闭式热泵干燥箱

Figure 1 Closed heat pump dryer

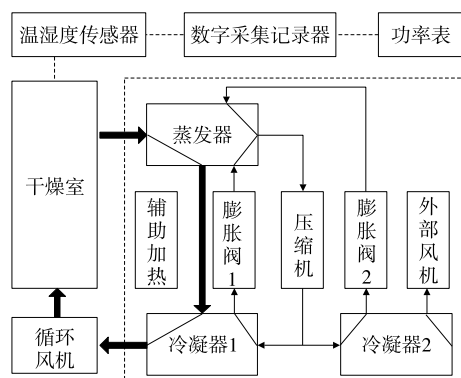


图 2 试验装置原理图

Figure 2 The schematic diagram of test device

膨胀阀 2、蒸发器组成冷媒外循环,实现干燥室多余热量的排出。干燥介质的热量传递给蒸发器,由冷媒经压缩机传递给冷凝器 2,外部风机推动大气带走冷凝器 2 的热量。热泵机组的内循环与外循环共同作用实现了干燥过程中各介质的温湿度控制。

数据采集记录装置由采集记录器、电能表、温度传感器、湿度传感器组成,周期性采集记录系统耗能与介质温湿度参数。温度传感器与湿度传感器放置于干燥室进风口;电能表与热泵系统的电源连接。

### 1.2 试验方法

取 40 cm×70 cm(长×宽)的纯棉布 15 片作为干燥物料,以保证试验物料属性均匀一致<sup>[12]</sup>。棉布复水后重量为(3 000±20) g。

(1) 能耗试验:基于果蔬等农产品常用干燥条件,设定干燥温度 60 ℃、相对湿度 10%,启动系统进行预热。待温湿度参数稳定后,将复水棉布平铺放入各干燥层,关闭干燥室门后计时开始。干燥开始后每 10 s 采集电能表、温度传感器、湿度传感器数据。蒸发器排出的冷凝液流入储水盒中,每 30 min 称量储水盒的质量。

(2) 干燥试验:设定干燥温度 60 ℃、相对湿度 10%,预热完毕后,将复水棉布放入干燥室内干燥计时开始。选定干燥室上、中、下 3 层料盘中物料为目标物料,间隔 30 min 称重一次,直至物料重量变化<0.02 g。

### 1.3 数据分析

1.3.1 系统能耗 热泵干燥的耗能部件包括控制系统、循环风机、热泵机组、辅助加热装置,其中控制系统和循环风机自干燥启动后持续运行,其能耗随干燥进行呈线性递增;而热泵机组与辅助加热装置受系统调控运行,其能耗通过对瞬时功率进行积分运算获得。干燥过程中物料在  $t$  时刻的过程能耗计算式<sup>[13]</sup>:

$$W = P_c t + P_f t + \int_0^t P_h dt + \int_0^t P_a dt , \quad (1)$$

式中:

$P_c$ ——控制系统功率,kW;

$P_f$ ——循环风机功率,kW;

$P_h$ ——热泵机组功率,kW;

$P_a$ ——辅助加热功率,kW;

$t$ ——干燥时间,h。

1.3.2 干燥特性 水分蒸发速率( $\dot{M}_w$ )是指干燥过程中单位时间物料蒸发水分的质量<sup>[14]</sup>。

$$\dot{M}_w = \frac{m_{wi} - m_{wi-1}}{(t_i - t_{i-1})}, \quad (2)$$

式中:

$\dot{M}_w$ ——物料的水分蒸发速率,kg/h;

$m_{wi}$ ——物料的实时重量,kg。

单位质量物料的水分蒸发速率( $\dot{R}_w$ )为:

$$\dot{R}_w = \frac{\dot{M}_w}{m_{w0}}, \quad (3)$$

式中:

$\dot{R}_w$ ——单位质量物料的水分蒸发速率,kg/(kg·h);

$m_{w0}$ ——物料的初始重量,kg。

蒸发器表面水蒸气冷凝速率( $\dot{R}_c$ )是指单位质量湿物料下热泵干燥过程中蒸发器表面水蒸气冷凝速率。

$$\dot{R}_c = \frac{m_{ci} - m_{ci-1}}{m_{w0}(t_i - t_{i-1})}, \quad (4)$$

式中:

$\dot{R}_c$ ——单位质量物料的冷凝速率,kg/(kg·h);

$m_{ci}$ ——冷凝水实时重量,kg。

1.3.3 能量利用分析 单位能耗除湿量(SMER)为消耗单位能量所除去物料中的水分量,则<sup>[15]</sup>:

$$SMER = \frac{m_{wi+1} - m_{wi}}{W_{i+1} - W_i}. \quad (5)$$

能量效率( $\eta$ )是指水分蒸发消耗的能量与系统总耗能的比值,则<sup>[16]</sup>:

$$\eta = \frac{h_1 \times (m_{wi+1} - m_{wi})}{3.6 \times 10^6 \times (W_{i+1} - W_i)}, \quad (6)$$

即:

$$\eta = \frac{h_1 \times SMER}{3.6 \times 10^6}, \quad (7)$$

式中:

$h_1$ ——水汽化潜热,J/g。

## 2 结果与分析

### 2.1 干燥特性

由图3可知,干燥箱内上、中、下3层料盘内物料的脱水速率存在明显差异,下层物料在干燥初期干燥速率最高,且呈降速干燥趋势;而上层物料干燥速率最低,且呈先升速后降速的趋势。这主要是干燥介质中的水蒸气随着流动方向逐渐积累,同时其温度下降,造成了空气介质的干燥能力沿气流方向逐渐降低<sup>[17]</sup>。

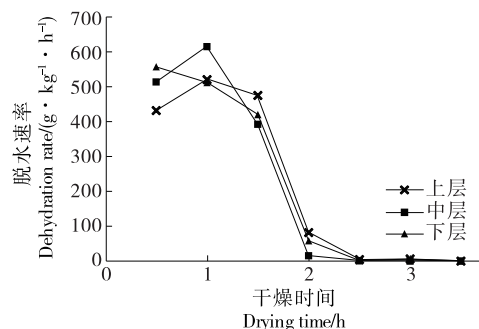


图3 热泵干燥的物料脱水速率曲线

Figure 3 The dehydration rate of materials during heat pump drying

由于不同位置的物料脱水速率差异较大,取各干燥层物料脱水速率的平均值进行热泵干燥物料脱水规律分析。由图4可知,物料表面水分蒸发速率与蒸发器表面的水蒸气冷凝速率随时间的演化规律一致,均呈先增长后下降的趋势,与 Hamid 等<sup>[18]</sup>的研究规律一致。物料脱水主要集中在干燥前 1.5 h, 脱除的水分占全过程的 96%;同时 88% 的水分经热泵机组排出系统。由于物料蒸发的部分水分滞留于空气介质与热泵机组中, 蒸汽冷凝的总量要低于物料水分蒸发量。

### 2.2 干燥介质温湿度变化

由图5可知,干燥开始后热泵机组将热量传递给空气介质而使其快速升温,温度由 40 °C 短时间提高至 50 °C。随后,介质温度升温速率放缓,80 min 后缓慢升高至目标温度(60 °C)上下波动,此阶段物料自身升温以及水分蒸发消耗大量的热量。物料表面蒸发出的水分在空气介质中积累而使其相对湿度值在干燥初期迅速提升,干燥 8 min 时达到 34.5%,随后受热泵机组除湿作用相对湿度持续下降。干燥前期介质相对湿度维持较高,可以显著提高物料升温速率,有助于物料表面水分的蒸发<sup>[19]</sup>。干燥 100 min 后,介质温度在 50~60 °C 范围内呈周期性的波动,主要是因为干燥后期热泵机组需要周

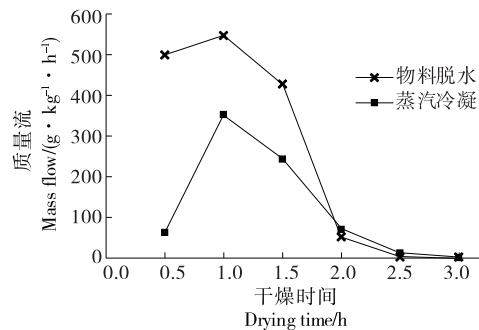


图4 物料水分蒸发与介质水分冷凝速率对比图

Figure 4 Comparison diagrams of water evaporation rate of material and water condensation rate of medium

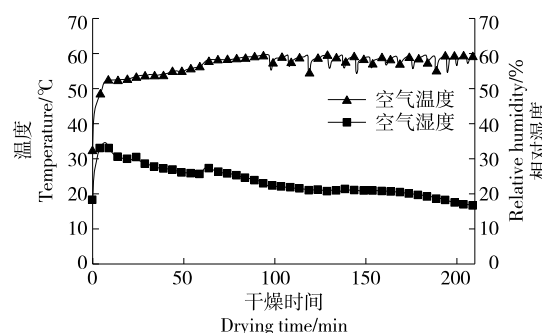


图 5 干燥过程中空气介质温湿度变化曲线

Figure 5 The variation curve of temperature and humidity of medium during drying process

期性地开启外部循环排出压缩机产生的多余热量,造成了大量的热量损失。

### 2.3 能量利用分析

由图 6 可知,干燥开始后,控制装置、循环风机、热泵机组、辅助加热管相继启动。控制装置、循环风机、热泵机组在干燥过程中持续运行。辅助加热管在持续运行 6 min 后停止,此时空气温度达到 50 °C(图 5)。干燥 100 min 时,外部风机开始间歇式启动,干燥室的热量通过冷凝器 2 排放至大气环境中。

由图 7(a)可知,热泵机组启动后的初始功率为 0.7 kW,

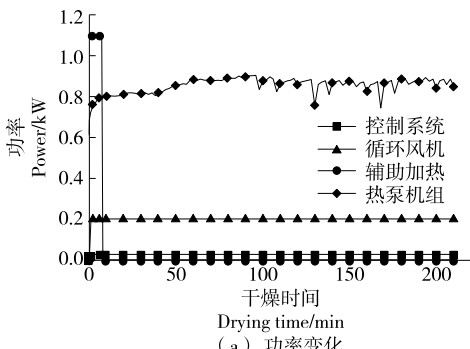


图 7 热泵干燥过程中各部件功耗变化曲线

Figure 7 The variation curve of component power consumption during heat pump drying process

温和介质升温所消耗的热量较少,热泵机组耗能主要完成湿空气冷凝换热。因此在 1.0 h 时,除湿能耗比具有最高值,能量效率可达 74.6%。干燥后期物料蒸发出的水分减少,空气介质的相对湿度降低,蒸发器表面水蒸气冷凝温度下降,因此除湿能耗比降低<sup>[22~23]</sup>。热泵机组在启动外部循环时不但持续消耗电量,而且会将大量热量排出大气环境中,进一步降低了能量的利用效率,干燥 2.0 h 后,除湿能耗比仅为 0.004 kg/kW。在低相对湿度控制方法下,干燥前期热泵干燥的除湿能耗比较高,后期除湿效率较低,不利于干燥机的节能,总除湿能耗比为 0.45 kg/kW,能量效率为 32.6%。

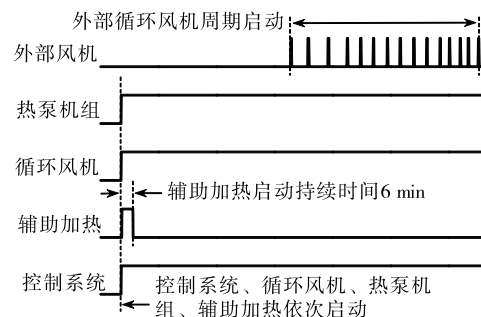


图 6 热泵干燥过程中各部件运行时序图

Figure 6 The sequence diagram of component operation during heat pump drying process

随着空气介质温度的提高,蒸发器负荷随之增大,压缩机排气温度提高而使功率缓慢上升至 0.85 kW<sup>[20~21]</sup>。干燥 90 min 后,热泵机组的功耗会出现周期性波动,此时外部循环开启,冷媒流经冷凝器 2 后返回压缩机。辅助加热工作时功率达到 1.0 kW,如图 7(b)所示,在干燥前 10 min 辅助加热消耗的能量高于热泵机组。干燥过程中热泵机组、循环风机持续运行,能量消耗分别占干燥过程总耗能的 75%,18%,为热泵干燥的主要耗能单元。

由图 8 可知,除湿能耗比在干燥过程中呈先升高后降低的趋势。干燥初期,热泵机组提供的热量大量用于物料升温和空气介质加热;而在 0.5~1.0 h 阶段,物料升

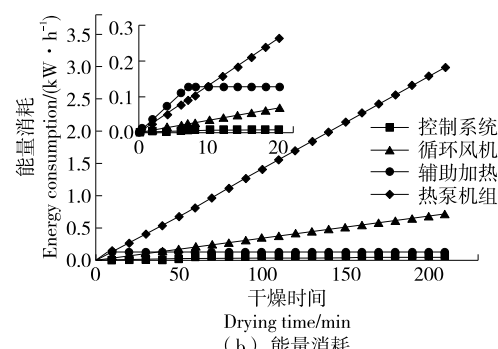


图 7 热泵干燥过程中各部件功耗变化曲线

Figure 7 The variation curve of component power consumption during heat pump drying process

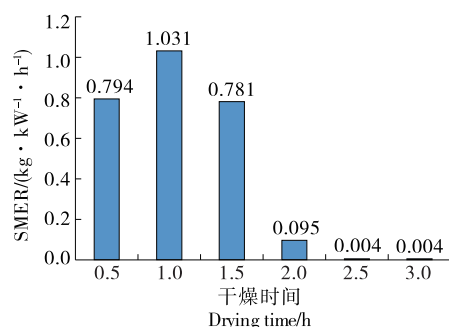


图 8 不同干燥时间段除湿能耗比对比图

Figure 8 Comparison diagram of the specific moisture extraction ratio in different drying stages

### 3 结论

探究了闭式热泵干燥的物料脱水、干燥介质状态、能耗的变化规律。结果表明,物料脱水与介质水蒸气冷凝集中发生于干燥前 1.5 h,此时,物料水分和干燥介质的相对湿度处于较高水平,热泵机组的除湿能耗比超过 0.78 kg/kW;干燥后期,干燥介质温度升高而相对湿度降低,热泵机组功耗增加但除湿速率下降,导致除湿能耗比降低至 0.1 以下。热泵机组是热泵干燥系统最高的耗能部件,单一的高温低湿的控制参数会造成热泵机组的持续运行,不利于后期的节能干燥。后续可进一步探究空气介质温湿度参数对闭式热泵干燥能量利用的作用机制,分析基于温湿度过程控制的节能调控方法,提高闭式热泵干燥的节能效果。

### 参考文献

- [1] SAGAR V R, SURESH K P. Recent advances in drying and dehydration of fruits and vegetables: A review [J]. *J Food Sci Technol*, 2010, 47: 15-26.
- [2] TUNCKAL C, DOYMAZ B. Performance analysis and mathematical modelling of banana slices in a heat pump drying system[J]. *Renewable Energy*, 2020, 150: 918-923.
- [3] 李阳春, 王剑锋, 陈光明, 等. 热泵干燥系统几种循环的对比分析与研究[J]. 农业机械学报, 2003, 34(6): 84-86, 95.
- LI C Y, WANG J F, CHEN G M, et al. Comparative analysis and study of several cycles of heat pump drying system[J]. *Transactions of the Chinese Society for Agricultural Machinery*, 2003, 34(6): 84-86, 95.
- [4] LIU H, YOUSAF K, CHEN K, et al. Design and thermal analysis of an air source heat pump dryer for food drying [J]. *Sustainability*, 2018, 10(9): 1-17.
- [5] 陈坤杰, 左毅, 李和清, 等. 热泵式低温循环谷物干燥机控制系统设计与试验[J]. 农业机械学报, 2021, 52(5): 316-323.
- CHEN K J, ZUO Y, LI H Q, et al. Design and experiment of heat pump low-temperature circulating grain dryer control system [J]. *Transactions of the Chinese Society for Agricultural Machinery*, 2021, 52(5): 316-323.
- [6] AKTAŞ M, TAŞERİ L, ŞEVIK S, et al. Heat pump drying of grape pomace: Performance and product quality analysis [J]. *Drying Technology*, 2019, 37(14): 1 766-1 779.
- [7] LI M, GUAN Z, GE Y, et al. Effect of pretreatment on water migration and volatile components of heat pump dried tilapia fillets [J]. *Drying Technology*, 2020, 38(14): 1 828-1 842.
- [8] PLOTEAU J P, NOEL H, FUENTES A, et al. Sludge convection drying process: Numerical modeling of a heat pump assisted continuous dryer[J]. *Drying Technology*, 2020, 38: 1 261-1 273.
- [9] BABU A K, KUMARESAN G, RAJ V A A, et al. Review of leaf drying: Mechanism and influencing parameters, drying methods, nutrient preservation, and mathematical models [J]. *Renewable & Sustainable Energy Reviews*, 2018, 90: 536-556.
- [10] JU H Y, ZHAO S H, MUJUMDAR A S, et al. Energy efficient improvements in hot air drying by controlling relative humidity based on Weibull and Bi-Di models [J]. *Food and Bioproducts Processing*, 2018, 111: 20-29.
- [11] TUNCKAL C, DOYMAZ I. Performance analysis and mathematical modelling of banana slices in a heat pump drying system[J]. *Renewable Energy*, 2020, 150: 918-923.
- [12] 王施平. 太阳能辅助热泵干燥监测系统设计与性能试验[D]. 南昌: 南昌航空大学, 2011: 48-51.
- WANG S P. Monitoring system design for solar-assisted heat pump drying and performance test[D]. Nanchang: Nanchang Hangkong University, 2011: 48-51.
- [13] 高东明, 罗钢. 干燥参数对苜蓿各含水率阶段干燥特性及能耗的影响 [J]. 江苏大学学报(自然科学版), 2020, 41(6): 685-693.
- GAO D M, LUO G. Effect of drying parameters on drying characteristics and energy consumption during alfalfa drying process [J]. *Journal of Jiangsu University (Natural Science Edition)*, 2020, 41(6): 685-693.
- [14] 孔令波. 纸页干燥过程传热传质数学模型的研究[D]. 广州: 华南理工大学, 2013: 23-24.
- KONG L B. Study on the mathematical model of heat and mass transfer in paper-drying process [D]. Guangzhou: South China University of Technology, 2013: 23-24.
- [15] 高萌, 李明, 王云峰, 等. 低温环境下热泵热风干燥藏药性能试验 [J]. 农业工程学报, 2020, 36(21): 316-322.
- GAO M, LI M, WANG Y F, et al. Experimental study on the performance for heat pump hot air drying of Tibetan medicine at low-temperature [J]. *Transactions of the Chinese Society of Agricultural Engineering*, 2020, 36(21): 316-322.
- [16] AMANTEA R P, FORTES M, FERREIRA W R, et al. Energy and exergy efficiencies as design criteria for grain dryers[J]. *Drying Technology*, 2017, 36(4): 140923.
- [17] 于贤龙. 基于介质湿度控制的胡萝卜热风节能干燥系统研究 [D]. 北京: 中国农业大学, 2020: 46-52.
- YU X L. Study of energy-saving hot air drying system for carrot based on drying medium humidity control strategy [D]. Beijing: China Agricultural University, 2020: 46-52.
- [18] HAMID K, SAJJAD U, YANG K S, et al. Assessment of an energy efficient closed loop heat pump dryer for high moisture contents materials: An experimental investigation and AI based modeling[J]. *Energy*, 2022, 238: 121819.
- [19] YU X L, ZIELINSKA M, JU H Y, et al. Multistage relative humidity control strategy enhances energy and exergy efficiency of convective drying of carrot cubes[J]. *International Journal of Heat and Mass Transfer*, 2020, 149: 119231.
- [20] 崔朝经, 黄金, 关军锋, 等. 梨片热泵干燥设备设计及干燥特性[J]. 食品工业, 2021, 42(9): 201-205.
- CUI C J, HUANG J, GUAN J F, et al. Design of heat pump drying equipment and drying characteristics of pear slice[J]. *The Food Industry*, 2021, 42(9): 201-205.

(下转第 181 页)

- 南药学, 2019, 17(6): 830-835.
- ZOU R, YAO H, HU J, et al. Preparation and quality evaluation of ursolic acid nanoemulsion[J]. Central South Pharmacy, 2019, 17 (6): 830-835.
- [12] QIU L, ZHAO X, ZU Y, et al. Ursolic acid nanoparticles for oral delivery prepared by emulsion solvent evaporation method: Characterization, in vitro evaluation of radical scavenging activity and bioavailability [J]. Artificial Cells, Nanomedicine, and Biotechnology, 2019, 47(1): 610-621.
- [13] 付亚玲, 高琳, 张东旭, 等. 齐墩果酸和熊果酸提取、分离与测定方法研究进展[J]. 食品研究与开发, 2020, 41(2): 196-199.
- FU Y L, GAO L, ZHANG D X, et al. Advances in extraction separation and determination of oleanolic acid and ursolic acid[J]. Food Research and Development, 2020, 41(2): 196-199.
- [14] ALVARADO H L, ABREGO G, SOUTO E B, et al. Nanoemulsions for dermal controlled release of oleanolic and ursolic acids: In vitro, ex vivo and in vivo characterization [J]. Colloids and Surfaces B-Biointerfaces, 2015, 130: 40-47.
- [15] KASHYAP D, TULI H S, SHARMA A K. Ursolic acid (UA): A metabolite with promising therapeutic potential[J]. Life Sciences, 2016, 146: 201-213.
- [16] 韩保庆. 紫苏油、亚麻籽油及熊果酸复合纳米乳体系的构建及性能研究[D]. 长春: 吉林大学, 2020: 4-9.
- HAN B Q. Construction and performance of perilla oil linseed oil and ursolic acid composite nanoemulsion system[D]. Changchun: Jilin University, 2020: 4-9.
- [17] 李春, 赵裕才, 陈晓倩, 等. 外水相中天然大分子对 W/O/W 型多重乳状液性质的影响 [J]. 中国食品学报, 2018, 18(12): 81-88.
- LI C, ZHAO Y C, CHEN X Q, et al. Effect of natural macromolecules of external aqueous phase on the properties of W/O/W type multiple emulsions[J]. Journal of Chinese Institute of Food Science and Technology, 2018, 18(12): 81-88.
- [18] 王可心, 段庆松, 王依凡, 等. 米糠蛋白 O/W 及 W/O/W 乳液制备及界面稳定性[J]. 食品科学, 2021, 42(22): 24-30.
- WANG K X, DUAN Q S, WANG Y F, et al. Preparation and interfacial stability of rice bran protein-stabilized O/W and W/O/W emulsions[J]. Food Science, 2021, 42(22): 24-30.
- [19] MEIRELLES A, COSTA A, CUNHA R L. Cellulosenanocrystals from ultrasound process stabilizing O/W Pickering emulsion[J]. International Journal of Biological Macromolecules, 2020, 158: 75-84.
- [20] 易醒, 罗俊溢, 骆叶晴, 等. 紫苏子油 O/W 型纳米微乳的制备及其氧化稳定性[J]. 中国食品学报, 2021, 21(4): 185-192.
- YI X, LUO J Y, LUO Y Q, et al. Preparation and oxidation stability of perilla seed oil O/W nano-emulsion [J]. Journal of Chinese Institute of Food Science and Technology, 2021, 21(4): 185-192.
- [21] ZHU Q M, QIU S, ZHANG H W, et al. Physical stability, microstructure and micro-rheological properties of water-in-oil-in-water (W/O/W) emulsions stabilized by porcine gelatin[J]. Food Chemistry, 2018, 253: 63-70.
- [22] BENETTI J V M, SILVA J T D, NICOLETTI V R. SPI microgels applied to pickering stabilization of O/W emulsions by ultrasound and high-pressure homogenization: Rheology and spray drying[J]. Food Research International, 2019, 122(AUG): 383-391.
- [23] 呼酩杰, 许虎君. 聚甘油脂肪酸酯 W/O/W 多重乳液的稳定性研究[J]. 日用化学工业, 2020, 50(5): 319-324.
- HU M J, XU H J. Study on the stability of polyglycerol fatty acid ester W/O/W multiple emulsion [J]. Modern Salt and Chemical Industry, 2020, 50(5): 319-324.
- [24] 丁玲, 唐艺华, 张丽芬, 等. 花生蛋白—果胶复合乳液凝胶的流变学特性和微观结构[J]. 食品科学, 2022, 43(16): 46-52.
- DING L, TANG Y H, ZHANG L F, et al. Rheological properties and microstructure of peanut protein-pectin composite emulsion gels[J]. Food Science, 2022, 43(16): 46-52.
- [25] 许馨予, 杨鸽隽, 贾斌, 等. 大豆分离蛋白—高酯柑橘果胶—没食子酸复合 Pickering 乳液制备及其稳定性分析[J]. 食品科学, 2022, 43(24): 42-51.
- XU X Y, YANG H J, JIA B, et al. Preparation and stability analysis of soy protein isolate-high methoxyl citrus pectin-gallic acid pickering emulsion[J]. Food Science, 2022, 43(24): 42-51.
- [26] ZHU C P, ZHANG H, HUANG G Q, et al. Whey protein isolate-low methoxyl pectin coacervates as a high internal phase Pickering emulsion stabilizer [J]. Journal of Dispersion Science and Technology, 2021, 42(7): 1 009-1 020.
- [27] ZHANG C, ZHU X X, ZHANG F P, et al. Improving viscosity and gelling properties of leaf pectin by comparing five pectin extraction methods using green tea leaf as a model material[J]. Food Hydrocolloids, 2020, 98(1): 112-132.

(上接第 98 页)

- [21] 蒋小强, 关志强, 谢晶, 等. 水产品热泵干燥装置性能参数的理论分析[J]. 农业工程学报, 2011, 27(S1): 373-376.
- JIANG X Q, GUAN Z Q, XIE J, et al. Analysis on performance parameters of heat pump drying system[J]. Transactions of the Chinese Society of Agricultural Engineering, 2011, 27 (S1): 373-376.
- [22] 吴耀森, 龚丽, 刘清化, 等. 加热型热泵干燥系统温湿度控制能力探讨[J]. 食品与机械, 2017, 33(10): 90-93.
- WU Y S, GONG L, LIU Q H, et al. Study on temperature and humidity control ability of heating type heat pump drying system [J]. Food & Machinery, 2017, 33(10): 90-93.
- [23] 曾文良, 陈柏霖, 陈萱, 等. 闭式热泵干燥系统的除湿特性试验[J]. 食品与机械, 2020, 36(11): 101-104.
- ZENG W L, CHEN B L, CHEN X, et al. Experimental investigation of dehumidification characteristics of closed drying system with heat pump [J]. Food & Machinery, 2020, 36 (11): 101-104.